

Quantum limit of hybrid atom-mechanical gyroscope based on electro-magnetically induced transparency

Sankar Davuluri^{1*} and Yong Li^{1,2}

¹*Beijing Computational Science Research Center, Beijing 100193, P. R. China and*

²*Synergetic Innovation Center for Quantum Effects and Applications,
Human Normal University, Changsha 410081, China.*

(Dated: April 21, 2022)

Application of hybrid atom-mechanical oscillator for absolute rotation detection is studied. The hybrid atom-mechanical oscillator consists of an atomic cell, filled with three level atoms, which is fixed on a mechanical oscillator. The atom-mechanical oscillator is placed on a rotating table such that the Coriolis force moves the atomic cell with respect to the incoming laser field. Thus the atomic resonance frequencies are Doppler shifted, and the phase of the laser field interacting with the atomic medium changes. Absolute rotation parameters are estimated by measuring the phase change in the laser field at the output of the atomic cell. Large dispersion is created in the atomic medium, using electromagnetically induced transparency, to enhance the phase change in the laser field interacting with the atomic medium. Contribution of the shot noise, the atomic noise and the noise due to the mechanical oscillation of the atomic cell are studied. We show that, under certain conditions, noise due to the mechanical oscillation of the atomic cell is on the same order of magnitude as the shot noise. The quantum limit of detectable rotation rate is estimated as 8.1×10^{-19} rad/s.

PACS numbers: 06.30.Gv, 42.50.Ct, 42.50.Nn, 42.50.Lc

Keywords: Electromagnetically induced transparency, quantum noise, hybrid atom-mechanical system

I. INTRODUCTION

Detection of absolute rotation has significant importance in fundamental physics [1, 2] and also in practical applications [3–5]. The most prominent methods for rotation detection are fiber optic gyroscopes [6] (FOG), ring laser gyroscopes [7] (RLG), matter wave interferometry [8, 9] with Sagnac effect [6, 7, 10, 11], and mechanical oscillators [12–14]. Here we propose an application of hybrid atom-mechanical oscillator for absolute rotation detection.

The hybrid atom-mechanical oscillator consists of an atomic cell which is mounted on a mechanical oscillator. The atomic cell is filled with three level atoms to create slow-light [15, 16] using electromagnetically induced transparency (EIT). The atom-mechanical oscillator is placed on a rotating table, and is driven co-sinusoidally along Y-axis. As a result, when the table rotates, the Coriolis force displaces the atomic cell along Z-axis. The motion of the atomic cell along Z-axis results in the Doppler shift in the atomic resonance frequencies with respect to the laser field which is propagating, along Z-axis, through the atomic cell. As a consequence, the phase of the laser field changes after interacting with the atomic medium. By measuring the phase change in the laser field at the output of the atomic cell, angular velocity of the rotating table can be estimated. In order to improve the phase sensitivity of the laser field interacting with atomic medium, we make the atomic medium dispersive [17], but transparent, by using the EIT [18–21]

phenomenon. Another advantage of working with EIT system is that its total quantum noise can set to be in the same order of magnitude as the shot noise [22] at the two-photon resonance for experimentally realizable parameters. Potential application of using EIT for rotation detection was described in [23], however a thorough investigation needs to be done.

Coming to the mechanical oscillator part, recent advances in the field of optomechanics [24, 25] demonstrate the design and control of high quality mechanical oscillators. We particularly consider a two-dimensional mechanical oscillator [26–28] which oscillates along Z-axis and Y-axis as shown in Fig. (2). The two-dimensional oscillator is driven co-sinusoidally along Y-axis. The frequency of the co-sinusoidal drive is chosen such that the Coriolis force acting on the oscillator, along Z-axis, is on resonance with the oscillator's frequency along Z-axis. This resonance condition ensures the optimal response of mechanical oscillator to the Coriolis force.

II. PRINCIPLE

For illustration purpose, assume that $\chi(\omega')$ is the frequency-dependent refractive index of the atomic medium mounted on a two-dimensional mechanical oscillator shown in Fig. (1). The laser source S, detector D, and the two-dimensional mechanical oscillator is fixed on a table (shown by grey rectangle in Fig. (1)) rotating with angular velocity $\dot{\theta}'$. When $\dot{\theta}' = 0$, change in the phase ϕ'_1 of the classical laser field after passing through

* sd3964@csrc.ac.cn

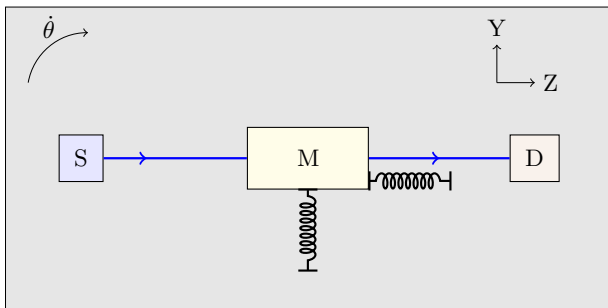


FIG. 1. A Laser source ‘S’ and a phase sensitive photo-detector ‘D’ are rigidly fixed with respect to each other on a table rotating with angular velocity θ . An optical medium ‘M’ with frequency dependent refractive index χ is mounted on a two-dimensional mechanical oscillator which is fixed to the rotating table. A classical electromagnetic field (shown with blue arrow) with frequency ω'_o passes through M.

the atomic medium is given as

$$\phi'_1 = \chi(\omega'_o)L'\frac{\omega'_o}{c}, \quad (1)$$

where $\omega'_o/2\pi$ is the frequency of the classical laser field, L' is the length of the atomic cell. The oscillator is driven co-sinusoidally along Y-axis at a frequency equal to the resonance frequency of the oscillator along Z-axis. As a result, when the table rotates with angular velocity θ' , the Coriolis force acting on the mechanical oscillator moves the atomic cell along Z-axis. Hence the laser frequency is Doppler shifted by ω'' with respect to the atomic resonance frequency. So when the table is rotating, change in the phase ϕ'_2 of the laser field after passing through the moving atomic medium is given as

$$\begin{aligned} \phi_2 &= \frac{L}{c}\chi(\omega'_o + \omega'')(\omega'_o + \omega'') \\ &= \frac{L'}{c}[\chi(\omega'_o)\omega'_o + \omega''(\chi(\omega'_o) + \omega'_o\frac{d\chi}{d\omega'}|_{\omega'=\omega'_o}) + \dots]. \end{aligned} \quad (2)$$

Assuming that non-linear dispersion in Eq. (2) is negligible, change in the phase of the laser field due to absolute rotation can be obtained from Eq. (1) and Eq. (2) as

$$\phi'_2 - \phi'_1 = \frac{L'}{c}[\omega''(\chi(\omega'_o) + \omega'_o\frac{d\chi}{d\omega'}|_{\omega'=\omega'_o})]. \quad (3)$$

Equation (3) shows that a larger linear dispersion of the atomic medium will enable us to measure smaller frequency shift ω'' . Since ω'' is a consequence of rotation, we can estimate the angular velocity of rotation from ω'' . Based on the idea presented in this section, we propose a hybrid atom-mechanical gyroscope in the next section.

III. EQUATIONS OF MOTION

Schematics of the atom-mechanical gyroscope are as shown in Fig. (2). An atomic-cell (shown by yellow rect-

angle in Fig. (2)) of length L is placed in the arm-1 of the Mach-Zehnder interferometer. The atomic cell is fixed on a mechanical oscillator (shown in green color in Fig. (2)) and we call this set-up as atom-mechanical oscillator. The atom-mechanical oscillator can oscillate along Z-axis with resonance frequency ν . The atom-mechanical oscillator is fixed on another platform (shown in brown color in Fig. (2)), we call this platform as driving platform, which is driven along Y-axis with mean velocity $\dot{y} = \dot{y}_o \cos(2\pi\nu t)$. Where t is time and \dot{y}_o is the maximum mean velocity of the driving platform. This complete set-up is placed on a platform (shown in grey color in Fig. (2)) rotating with angular velocity θ .

Atoms inside the atomic cell are three-level atoms with energy of each atomic level $|u\rangle (u = a, b, c)$ given by $\hbar\omega_u$, where \hbar is the reduced Planck constant and $\omega_u/2\pi$ is the frequency. The energy level structure of the atoms inside the atomic cell is shown in big yellow circle is Fig. (2). Transition $|b\rangle - |c\rangle$ is electric-dipole forbidden. Transition $|a\rangle - |b\rangle$, with electric-dipole moment \wp_{ab} , is coupled to the weak quantum probe field (shown in blue color in Fig. (2)) propagating along Z-axis in the arm-1 of the interferometer. Transition $|a\rangle - |c\rangle$, with dipole moment \wp_{ac} , is driven by a strong classical laser field for which the cross-section area is shown by the red circle in Fig. (1). The classical drive field has frequency $\omega_d/2\pi$ and is propagating perpendicular to the YZ-plane (see Fig. (2)). We assume that the diameter L_d of both probe and drive laser fields is larger than \dot{y}_o/ν , so that the number of atoms in the laser-atom interaction region do not change because of the driving platform’s oscillation along Y-axis. This condition can easily be satisfied for realistic parameters like $L_d = 2 \times 10^{-2}$ m, $\dot{y}_o = 10^{-2}$ m/s and $\nu = 1$ Hz.

By setting $\dot{\theta} = 0$ and $\dot{y} = 0$, propagation [29] of quantum electromagnetic field is described by using multi-mode description [30]. Hence we consider the quantum probe field coupling with $|a\rangle - |b\rangle$ transition as the quasi-monochromatic field, represented by $\sum_r \hat{c}_r$, with mean wave-vector k_p . The wave vector for the r -th mode of the probe field is

$$k_r = k_p + \frac{2r\pi}{L_q}, \quad \omega_r = \omega_p + \frac{2r\pi c}{L_q}, \quad r = -R, \dots, R, \quad (4)$$

where c is the velocity of light in vacuum, $\omega_r = ck_r$, $\omega_p = ck_p$, and L_q is the quantization length so that the quantization volume is AL_q with A as the area of cross section of electromagnetic field to be quantized. Interaction between the quantum field and the atoms in a sample of length L can be described by using the technique described in Refs. [22, 31–33]. So we divide the total interaction length L into $(2P + 1)$ sub-cells. Each sub-cell is centered at $z_l = lL/(2P + 1)$, $l = -P, \dots, P$, such that $\Delta z := z_{l+1} - z_l = L/(2P + 1)$. Single-atom operators are represented by $\hat{\sigma}_{uv}^{ls} = |u\rangle^{ls}\langle v|^{ls}$, where $v = a, b, c$, superscripts s and l denote the s -th atom in the l -th sub-cell centered at z_l . Hence the Hamiltonian for atom-field

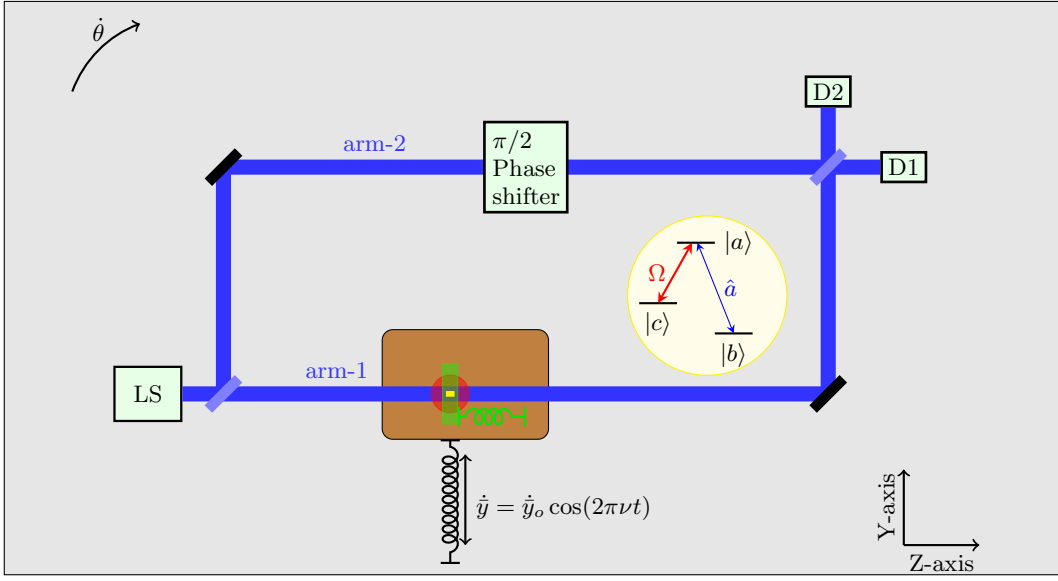


FIG. 2. LS: Laser source, D1,D2: photo detector. The small yellow rectangle represents cold (temperature of atoms $T_a = 10^{-6}$ K) atomic cell which is fixed on a mechanical oscillator shown in green color. We call this set-up of atomic-cell fixed on the mechanical oscillator as atom-mechanical oscillator. The atom-mechanical oscillator can oscillate along Z-axis and its resonance frequency is ν . The brown rectangle represent the driving platform on which the atom-mechanical oscillator is fixed. The driving platform is driven along Y-axis with velocity $\dot{y} = \dot{y}_o \cos(2\pi\nu t)$, where t is time and \dot{y}_o is maximum mean velocity along Y-axis, so that the number of atoms in the laser-atom interaction region do not change because of the driving platform's oscillation along Y-axis. The complete set-up is fixed on a platform (the big grey rectangle) rotating with angular velocity $\dot{\theta}$. The Z-axis and Y-axis shown in the figure are fixed with respect to the rotating platform. When $\dot{\theta} \neq 0$ the atom-mechanical cell moves along the Z-axis with velocity \dot{z}_m , \hat{z}_m is center of mass of the atom-mechanical oscillator, because of the Coriolis force acting on it. As a result the resonance frequency of the atoms in the atom-mechanical oscillator are Doppler shifted with respect to the probe laser. This rotation induced Doppler frequency shift leads to phase shift which is measured at D1 and D2 to estimate $\dot{\theta}$.

interaction, when $\dot{\theta} = 0$ and $\dot{y} = 0$, is given as

$$\hat{H} = (\hbar \sum_{s,l,r} g_r \hat{\sigma}_{ab}^{ls} \hat{c}_r e^{i(k_r - k_p)z_l} + \sum_{l,s} \hbar \tilde{\Omega} \hat{\sigma}_{ac}^{ls} + \text{HC}) + \sum_r \hbar \omega_r (\hat{c}_r^\dagger \hat{c}_r + \frac{1}{2}) + \sum_{l,s,u} \hbar \omega_u \hat{\sigma}_{uu}^{ls}, \quad (5)$$

where HC is the Hermitian conjugate, $\tilde{\Omega} = -\varphi_{ac} E_d e^{-i\omega_d t} / \hbar$ with E_d being the amplitude of the drive field, $g_r = -(\varphi_{ab} / \hbar) \sqrt{\hbar \omega_r / \epsilon_o A L_q}$. In the limit $L_q \rightarrow \infty$ and $\Delta z \rightarrow 0$, by defining

$$\frac{2R+1}{N} \sum_s \hat{\sigma}_{uv}^{ls} |_{z_l \rightarrow z} := \hat{\sigma}_{ij}^o, \quad (6a)$$

$$\frac{2R+1}{N} \sum_s \hat{F}_{uv}^{ls} |_{z_l \rightarrow z} := \hat{F}_{ij}^o,$$

$$\frac{1}{\sqrt{2\pi}} \int_0^\infty d\omega \hat{c}(\omega) e^{-i\omega t} e^{i(k - k_p)z_l} |_{z_l \rightarrow z} := \hat{a} e^{-i\omega_p t},$$

equations of motion (refer Appendix. (A) for more details) for the quantum field and the atomic operators are

given as

$$\left(\frac{\partial}{\partial t} + c \frac{\partial}{\partial z} \right) \hat{a} = -i N g_c^* \frac{c}{L_q} \hat{\sigma}_{ba}, \quad (7a)$$

$$\dot{\hat{\sigma}}_{ba} = [i(-\omega_{ab} + \omega_p) - \gamma_{ab}] \hat{\sigma}_{ba} + i g_c (\hat{\sigma}_{aa} - \hat{\sigma}_{bb}) \hat{a} - i \Omega \hat{\sigma}_{bc} + \hat{F}_{ba}, \quad (7b)$$

$$\dot{\hat{\sigma}}_{bc} = [i(-\omega_{cb} + (\omega_p - \omega_d)) - \gamma_{bc}] \hat{\sigma}_{bc} + i g_c \hat{\sigma}_{ac} \hat{a} - i \Omega \hat{\sigma}_{ba} + \hat{F}_{bc}, \quad (7c)$$

$$\dot{\hat{\sigma}}_{ac} = [i(\omega_{ac} - \omega_d) - \gamma_{ac}] \hat{\sigma}_{ac} + i(\hat{\sigma}_{cc} - \hat{\sigma}_{aa}) \Omega + i g_c^* \hat{\sigma}_{bc} \hat{a}^\dagger + \hat{F}_{ac}, \quad (7d)$$

where $g_c = -\varphi_{ab} / \hbar (\sqrt{\hbar \omega_p / \epsilon_o A c})$, $\omega_{uv} = \omega_u - \omega_v$, $\Omega = -\varphi_{ac} E_d / \hbar$ is taken as a real quantity, γ_{uv} is the de-coherence between the atomic levels $|u\rangle$ and $|v\rangle$, $\hat{\sigma}_{uv}$ and \hat{F}_{uv} are the rotating wave approximated operators of $\hat{\sigma}_{uv}^o$ and \hat{F}_{uv}^o , respectively. Even though the transition $|b\rangle - |c\rangle$ is electric dipole forbidden, other factors like line-width of the drive laser lead to decoherence on $|b\rangle - |c\rangle$

transition. Hence we assumed phenomenological γ_{bc} in Eq. (7c).

For $\dot{\theta} \neq 0$ and $\dot{y} = \dot{y}_o \cos(2\pi\nu t)$, a classical Coriolis force of $2m\dot{y}_o\dot{\theta} \cos(2\pi\nu t)$ is exerted on the atom-mechanical oscillator cell, along the Z-axis, when the table rotates with angular velocity $\dot{\theta}$. Equation of motion of the atom-mechanical oscillator along Z-axis is given as

$$\ddot{\hat{z}}_m + \frac{\nu}{Q}\dot{\hat{z}}_m + (2\pi\nu)^2\hat{z}_m = 2\dot{y}_o\dot{\theta} \cos(2\pi\nu t) + \hat{F}_{th}, \quad (8)$$

where Q and \hat{z}_m are the quality factor and center of mass position of the atom-mechanical oscillator, respectively. \hat{F}_{th} is the thermal noise operator. Substituting the ansatz $\hat{z}_m = \hat{z}_{m0} \cos(2\pi\nu t)$ in Eq. (8) gives

$$\dot{\hat{z}}_m = \frac{2Q\dot{y}_o\dot{\theta}}{\nu} \cos(2\pi\nu t) + \frac{Q}{\nu}\hat{F}_{th}. \quad (9)$$

As the atomic cell is moving with velocity $\dot{\hat{z}}_m$ with respect to the laser fields, resonance frequencies of the atomic energy levels are shifted due to the Doppler effect as

$$\omega_{ab} \rightarrow \omega_{ab}(1 - \frac{\dot{\hat{z}}_m}{c}). \quad (10)$$

By substituting Eq. (10) in Eq. (7), and by setting $\omega_p = \omega_{ab}$ and $\omega_d = \omega_{ac}$, we can write

$$\left(\frac{\partial}{\partial t} + c\frac{\partial}{\partial z}\right)\hat{a} = -iNg_c^* \frac{c}{L_q}\hat{\sigma}_{ba}, \quad (11a)$$

$$\dot{\hat{\sigma}}_{ba} = (i\omega_{ab}\frac{\dot{\hat{z}}_m}{c} - \gamma_{ab})\hat{\sigma}_{ba} + ig_c(\hat{\sigma}_{aa} - \hat{\sigma}_{bb})a - i\Omega\hat{\sigma}_{bc} + \hat{F}_{ba}, \quad (11b)$$

$$\dot{\hat{\sigma}}_{bc} = (i\omega_{ab}\frac{\dot{\hat{z}}_m}{c} - \gamma_{bc})\hat{\sigma}_{bc} + ig_c\hat{\sigma}_{ac}a - i\Omega\hat{\sigma}_{ba} + \hat{F}_{bc}, \quad (11c)$$

$$\dot{\hat{\sigma}}_{ac} = (-\gamma_{ac})\hat{\sigma}_{ac} + i(\hat{\sigma}_{cc} - \hat{\sigma}_{aa})\Omega + ig_c^*\hat{\sigma}_{bc}\hat{a}^\dagger + \hat{F}_{ac}. \quad (11d)$$

Note that the $\dot{\hat{z}}_m$ in Eq. (11) has the information about $\dot{\theta}$ as given in Eq. (9).

A. Signal

Equations (11) are linearized by writing operators as $\hat{\sigma}_{uv} = \bar{\sigma}_{uv} + \hat{\delta}_{uv}$, and $\hat{a} = \bar{a} + \hat{\delta}$, with $\bar{\sigma}_{uv}$, $\hat{\delta}_{uv}$, \bar{a} , and $\hat{\delta}$ as the classical mean of $\hat{\sigma}_{uv}$, quantum fluctuation in $\hat{\sigma}_{uv}$, classical mean of \hat{a} and quantum fluctuation in \hat{a} , respectively. Vacuum field entering arm-1 is included in $\hat{\delta}$. Assuming EIT conditions, we treat \hat{a} only up to its first order while Ω is kept to all orders. Most of the atomic population stays in $|b\rangle$ under EIT conditions. Hence, we can write [34, 35] $\hat{\sigma}_{bb}^0 = 1$ and $\hat{\sigma}_{aa}^0 = \hat{\sigma}_{cc}^0 = \hat{\sigma}_{ac}^0 =$

0 (the superscript '0' indicates zeroth order in \hat{a} , while the superscript '1' indicates first order in \hat{a}). For realistic parameters: $\gamma_{ab} \approx \gamma_{ac} \approx 10^7$ Hz, while $\nu \approx 1$ Hz. Because $\nu \ll \gamma_{ab} \approx \gamma_{ac}$, by using adiabatic approximation[36], $\bar{\sigma}_{ba}^1$ is evaluated as

$$\bar{\sigma}_{ba}^1 = \frac{ig_c\bar{a}(i\omega_{ab}\frac{\dot{\hat{z}}_m}{c} - \gamma_{bc})}{(i\omega_{ab}\frac{\dot{\hat{z}}_m}{c} - \gamma_{ab})(i\omega_{ab}\frac{\dot{\hat{z}}_m}{c} - \gamma_{bc}) + \Omega^2}, \quad (12)$$

where $\dot{\hat{z}}_m = 2\dot{y}_o\dot{\theta} \cos(2\pi\nu t)Q/\nu$. Using Eq. (12), the propagation of steady state probe field \bar{a} is given[37] as

$$\frac{\partial}{\partial z}\bar{a} = \Lambda_o\bar{a}, \quad (13)$$

where

$$\Lambda_o = \kappa \frac{i\omega_{ab}\frac{\dot{\hat{z}}_m}{c} - \gamma_{bc}}{(i\omega_{ab}\frac{\dot{\hat{z}}_m}{c} - \gamma_{ab})(i\omega_{ab}\frac{\dot{\hat{z}}_m}{c} - \gamma_{bc}) + \Omega^2},$$

with $\kappa = N|g|^2/c$, and $g = g_c\sqrt{c/L_q}$. Solving Eq. (13) gives

$$\bar{a}(L) = \bar{a}_o e^{\Lambda_o L}, \quad (14)$$

where $\bar{a}_o = \bar{a}(z=0)$. Assuming that $\Omega^2 \gg \gamma_{ab}\gamma_{bc}$, and by considering $\omega_{cb}\dot{\hat{z}}_m/c$ and $\omega_{ab}\dot{\hat{z}}_m/c$ upto their first order only, Λ_o can be approximated as

$$\Lambda_o \approx \kappa \left(-\frac{\gamma_{bc}}{\Omega^2} + i\frac{\omega_{ab}\frac{\dot{\hat{z}}_m}{c}}{\Omega^2} \right). \quad (15)$$

Electromagnetic field in the arm-2 of Fig. (2) is represented by \hat{a}_1 . Hence the difference in the photo detector readings, after adding a constant $\pi/2$ phase[38] to \hat{a}_1 , is given as

$$\hat{I}_1 - \hat{I}_2 = \hat{a}^\dagger \hat{a}_1 + \hat{a} \hat{a}_1^\dagger. \quad (16)$$

The mean difference in the photo-detector readings is given as

$$\langle \hat{I}_1 - \hat{I}_2 \rangle = \bar{a}^* \bar{a}_1 + \bar{a} \bar{a}_1^*, \quad (17)$$

where $\bar{a}_1 = \hat{a}_1 - \hat{\delta}_1$ with $\hat{\delta}_1$ as quantum fluctuation in \hat{a}_1 . Vacuum field entering arm-2 is included in $\hat{\delta}_1$. By using the relation $\bar{a}(z_o) = -i\bar{a}_1$ and using Eq. (9), Eq. (15), and Eq. (14), we can write Eq. (17) as

$$\langle I_1 - I_2 \rangle \approx -\frac{2|\bar{a}|^2 2\dot{y}_o\dot{\theta}}{\nu/Q} e^{-\frac{\kappa\gamma_{bc}}{\Omega^2}L} \left(\frac{\kappa\omega_{ab}}{c\Omega^2}L \right) \cos(2\pi\nu t). \quad (18)$$

Minimizing Eq. (18) with respect to $\kappa\gamma_{bc}L/\Omega^2$ shows that we obtain maximum signal when $\kappa\gamma_{bc}L = \Omega^2$. At $\Omega^2 = \kappa\gamma_{bc}L$, signal is given as

$$\langle I_1 - I_2 \rangle = -\frac{4|\bar{a}|^2 \dot{y}_o\dot{\theta}}{\nu/Q} e^{-1} \left(\frac{\omega_{ab}}{c\gamma_{bc}} \right) \cos(2\pi\nu t). \quad (19)$$

Signal in Eq. (19) represents the number of photons detected per unit time. Hence the total number of photons detected in a measurement time of t_m is given as

$$\int_{t_o}^{t_o+t_m} \langle I_1 - I_2 \rangle dt. \quad (20)$$

Assuming that $t_m \ll 1/\nu$ and considering that $t_o = 0$, we can simplify Eq. (20) as

$$S_o := \int_0^{t_m} \langle I_1 - I_2 \rangle dt = \frac{4\dot{y}_o \dot{\theta} \omega_{ab}}{c \gamma_{bc} \nu / Q} \frac{P t_m}{\hbar \omega_p} e^{-1}, \quad (21)$$

where P is the power of the probe field. Since $t_m \ll 1/\nu$, there is no significant change in velocity of the atomic cell during the time of measurement. Hence, the system behaves as if atomic cell is moving with constant velocity, which is equal to the velocity at t_o , with respect to the incoming electromagnetic field. For $t_m \ll 1/\nu$, it is enough to consider the effect of ν up to its first order.

IV. NOISE SPECTRUM

Shot noise, atomic noise, and mechanical noise of the atom-mechanical oscillator are the three major sources of noise in the hybrid atom-mechanical system. Noise from the mechanical motion of the atomic cell is given by \hat{F}_{th} term in Eq. (9). By substituting Eq. (9) in Eq. (11), the linearized equations of motion for the fluctuations are

$$\left(\frac{\partial}{\partial t} + c \frac{\partial}{\partial z} \right) \hat{\delta} = -i N g_c^* \frac{c}{L_q} \hat{\delta}_{ba}^1, \quad (22a)$$

$$\hat{\delta}_{ba}^1 = (i \omega_{ab} \frac{\dot{z}_m}{c} - \gamma_{ab}) \hat{\delta}_{ba}^1 - i g_c \hat{a} - i \Omega \hat{\delta}_{bc}^1 + \hat{F}_{ba} + \hat{T}_{ba}, \quad (22b)$$

$$\hat{\delta}_{bc}^1 = (i \omega_{ab} \frac{\dot{z}_m}{c} - \gamma_{bc}) \hat{\delta}_{bc}^1 - i \Omega^* \hat{\delta}_{ba}^1 + \hat{F}_{bc} + \hat{T}_{bc}. \quad (22c)$$

where $\hat{T}_{ba} = i \frac{\omega_{ab} \hat{F}_{th}}{c \nu / Q} \bar{\sigma}_{ba}$ and $\hat{T}_{bc} = i \frac{\omega_{ab} \hat{F}_{th}}{c \nu / Q} \bar{\sigma}_{bc}$. The terms $\omega_{ab} \dot{z}_m / c$, $\omega_{cb} \dot{z}_m / c$, $\hat{\delta}_{cb}^1$, and $\hat{\delta}_{ab}^1$ are very small, hence the product terms such as $i \omega_{ab} \dot{z}_m \hat{\delta}_{bc}^1 / c$ and $i \omega_{ab} \dot{z}_m \hat{\delta}_{ab}^1 / c$, can be neglected in Eq. (22). By using the Fourier transform function $\mathfrak{F}(x(t)) = \frac{1}{\sqrt{2\pi}} \int_{-\infty}^{\infty} x(t) e^{i\omega t} dt$, Eq. (22a) can be written as

$$\frac{\partial}{\partial z} \hat{\delta}(z, \omega) = i \frac{\omega}{c} - i \frac{N g_c^*}{c} \frac{c}{L_q} \hat{\delta}_{ba}^1(z, \omega), \quad (23)$$

where $\hat{\delta}_{ba}^1(z, \omega)$ can be obtained by solving Eq. (22) in the frequency domain. Solving Eq. (23) gives fluctuation

in the field at the output of the atomic cell as

$$\hat{\delta}(L, \omega) = \hat{\delta}_o(\omega) e^{\Lambda L} + \int_0^L e^{-\Lambda(z_1-L)} (\hat{F}(z_1, \omega) + \hat{T}(z_1, \omega)) dz_1, \quad (24)$$

where $\hat{\delta}_o(\omega) = \hat{\delta}(z=0, \omega)$,

$$\hat{F}(z_1, \omega) = \frac{N g_c^*}{c} \frac{c}{L_q} \frac{-\Omega \hat{F}_{bc}(z_1, \omega) + i \hat{F}_{ba}(z_1, \omega)}{(i\omega - \eta_{ba}) + \frac{\Omega^2}{(i\omega - \gamma_{bc})}},$$

$$\hat{T}(z_1, \omega) = \frac{N g_c^*}{c} \frac{c}{L_q} \frac{-\Omega \hat{T}_{bc}(z_1, \omega) + i \hat{T}_{ba}(z_1, \omega)}{(i\omega - \eta_{ba}) + \frac{\Omega^2}{(i\omega - \gamma_{bc})}}$$

and

$$\Lambda(\omega) = i \frac{\omega}{c} + \kappa \frac{1}{(i\omega - \eta_{ba}) + \frac{\Omega^2}{i\omega - \gamma_{bc}}}. \quad (25)$$

The first term on the RHS of Eq. (24) gives shot noise, while the second term gives atomic noise and the third term gives noise due to the mechanical motion of the atom-mechanical oscillator. Fluctuation in Eq. (16), denoted by $\hat{\Delta}$, is given as

$$\hat{\Delta} = \hat{I}_1 - \hat{I}_2 - \langle \hat{I}_1 - \hat{I}_2 \rangle = \hat{\delta}_1^\dagger \bar{a} + \hat{\delta}_1 \bar{a}^* + \hat{\delta}^\dagger \bar{a}_1 + \hat{\delta} \bar{a}_1^*. \quad (26)$$

Variance of $\hat{\Delta}(\omega)$, where $\hat{\Delta}(\omega) = \mathfrak{F}(\hat{\Delta})$, is given as

$$\langle \hat{\Delta}^\dagger(\omega) \hat{\Delta}(\omega') \rangle = (V_t + V_a) \delta(\omega + \omega'), \quad (27)$$

where V_t , and V_a are the power spectral densities of noise due to the EIT system and noise due to the mechanical motion of the atom-mechanical oscillator, respectively. In the next two subsections, we estimate the noise due to EIT and mechanical motion of the atom-mechanical oscillator.

A. Noise due to EIT system

By defining $\hat{\delta}_a(z, \omega)$ as the fluctuation in the field at the output of the atomic cell due to EIT system, from Eq. (24), we can write

$$\hat{\delta}_a(L, \omega) = \hat{\delta}_o(\omega) e^{\Lambda L} + \int_0^L e^{-\Lambda(z_1-L)} \hat{F}(z_1, \omega) dz_1, \quad (28)$$

Noise in the EIT system can be estimated by calculating $\langle \hat{\Delta}_a^\dagger(\omega) \hat{\Delta}_a(\omega') \rangle$, where $\hat{\Delta}_a(\omega) = (\hat{\delta}_a(L, \omega) \bar{a}_1^* + \hat{\delta}_a^\dagger(L, -\omega) \bar{a}_1)$. Substituting Eq. (28) in $\hat{\Delta}_a(\omega)$, and by using the correlation functions

$$\langle \hat{F}_{bc}(t_1, z_1) \hat{F}_{bc}^\dagger(t_2, z_2) \rangle = 2\gamma_{bc} \delta(t_1 - t_2) \delta(z_1 - z_2) \frac{L_q}{N},$$

$$\langle \hat{F}_{ba}(t_1, z_1) \hat{F}_{ba}^\dagger(t_2, z_2) \rangle = 2\gamma_{ba} \delta(t_1 - t_2) \delta(z_1 - z_2) \frac{L_q}{N},$$

$$\langle \hat{\delta}_o(t) \hat{\delta}_o^\dagger(t') \rangle = \langle \hat{\delta}_1(t) \hat{\delta}_1^\dagger(t') \rangle = \delta(t - t').$$

we can write

$$V_a = |\bar{a}|^2 + \left(e^{2\Lambda'L} + \kappa \frac{1 - e^{-2\Lambda'L}}{-2\Lambda'} \frac{\Omega^2(-2\gamma_{bc}) + |\gamma_{bc}|^2(-2\eta_{ba})}{(i\omega - \eta_{ba})(i\omega - \gamma_{bc}) + \Omega^2} \right) |\bar{a}_1|^2, \quad (29)$$

where Λ' is the real part of Λ . The first two terms on the RHS of Eq. (29) represent the effect of shot noise, while the last term comes from the atomic noise. Because the signal in Eq. (18) is oscillating with frequency ν , we are interested in finding the noise component at $\omega = 2\pi\nu$. However, we assume that ν is much less than the bandwidth of EIT window, also the signal in Eq. (21) is evaluated under the condition $t_m \ll \nu$. Hence we do a Taylor expansion of Eq. (29) and keep the terms only up to the first order of ν . Substituting Eq. (25) and Eq. (14) in Eq. (29), at $\Omega^2 = \kappa\gamma_{bc}L$, we obtain

$$V_1 = |\bar{a}_o|^2(1 + e^{-2}), \quad (30)$$

where V_1 is power spectral density of noise due to EIT

system when $\Omega^2 = \kappa\gamma_{bc}L$.

B. Noise due to mechanical oscillator

We define $\hat{\delta}_t$ as the fluctuation in the field, at the output of the atomic cell, due to \hat{F}_{th} . From Eq. (24), we can write

$$\hat{\delta}_t(L, \omega) = \int_0^L e^{-\Lambda(z_1-L)} \hat{T}(z_1, \omega) dz_1 \quad (31)$$

Substituting $\hat{T}_{ba} = i\frac{\omega_{ab}\hat{F}_{th}}{c\nu/Q}\bar{\sigma}_{ba}$ and $\hat{T}_{bc} = i\frac{\omega_{ab}\hat{F}_{th}}{c\nu/Q}\bar{\sigma}_{bc}$, in Eq. (31) and by using the relation $\bar{\sigma}_{bc} = i\Omega^*\bar{\sigma}_{ba}/(i\omega_{cb}\dot{z}/c - \gamma_{bc})$, we can write that

$$\hat{\delta}_t(L, \omega) = \frac{Ng_c}{c} \frac{c}{L_q} \frac{\left(\frac{\omega_{ab}\Omega^2}{(i\omega_{cb}\dot{z}/c - \gamma_{bc})(i\omega - \gamma_{bc})} - \omega_{ab} \right) \frac{\hat{F}_{th}(\omega)}{c\nu/Q} \int_0^L e^{-\Lambda(z_1-L)} \bar{\sigma}_{ba}(z_1) dz_1}{(i\omega - \eta_{ba} + \frac{\Omega^2}{i\omega - \gamma_{bc}})}, \quad (32)$$

From Eq. (12) and Eq. (14), we can write

$$\int_0^L e^{\Lambda(L-z_1)} \bar{\sigma}_{ba}(z_1) dz_1 = \frac{ig_c\Lambda_o e^{\Lambda L}}{\kappa} \int_0^L e^{(\Lambda_o - \Lambda)z_1} \bar{a}_o dz_1 \approx \frac{ig_c\Lambda_o}{\kappa} \bar{a}_o e^{\Lambda L} L. \quad (33)$$

By substituting Eq. (33) in Eq. (32), noise due to \hat{F}_{th} can be estimated by calculating $\langle \hat{\Delta}_t^\dagger(\omega) \hat{\Delta}_t(\omega') \rangle$, where

$$\hat{\Delta}_t(\omega) = (\hat{\delta}_t(L, \omega) \bar{a}_1^\dagger + \hat{\delta}_t^\dagger(L, -\omega) \bar{a}_1).$$

$$\begin{aligned} \langle \hat{\Delta}_t^\dagger(\omega) \hat{\Delta}_t(\omega') \rangle &= \left| \frac{\Omega^2 \Lambda_o e^{\Lambda L}}{(i\omega_{cb}\dot{z}/c - \gamma_{bc})(i\omega - \gamma_{bc})} - 2\Lambda_o e^{\Lambda L} + \frac{\Omega^2 \Lambda_o^* e^{\Lambda^* L}}{(-i\omega_{cb}\dot{z}/c - \gamma_{bc})(i\omega - \gamma_{bc})} - 2\Lambda_o^* e^{\Lambda^* L} \right|^2 \\ &\quad \times \left| \frac{\omega_{cb} \bar{a}_1}{(i\omega - \eta_{ba}) + \frac{\Omega^2}{i\omega - \gamma_{bc}}} \right|^2 \langle \hat{F}_{th} \hat{F}_{th} \rangle \left(\frac{Q}{c\nu} \right)^2 |\bar{a}_o|^2 = V_t \delta(\omega + \omega'). \end{aligned} \quad (34)$$

Applying the Taylor expansion on Eq. (34) and keeping the terms up to the first order of ν and \dot{z}_m , and using the correlation function

$$\langle \hat{F}_{th}(\omega) \hat{F}_{th}(\omega') \rangle = \frac{h\nu^2}{Qm} \left(1 + \frac{2}{e^{h\nu/k_B T} - 1} \right) \delta(\omega + \omega'),$$

where h is Planck constant, m is effective mass of atom-mechanical oscillator, k_B is the Boltzmann constant, T is the temperature of the mechanical oscillator along Z-axis,

we can simplify V_t as

$$V_t \approx 4|\bar{a}_o|^4 \frac{Q\omega_{ab}^2 h}{c^2 \gamma_{bc}^2 m} \left(1 + \frac{2}{e^{h\nu/k_B T} - 1} \right) e^{-2}. \quad (35)$$

We used the condition $\Omega^2 = \kappa\gamma_{bc}L$ in Eq. (35). For

$$4|\bar{a}_o|^2 \frac{Q\omega_{ab}^2 h}{c^2 \gamma_{bc}^2 m} \left(1 + \frac{2}{e^{h\nu/k_B T} - 1} \right) = 1, \quad (36)$$

the noise due to the mechanical motion of the atomic cell is in the same order of magnitude as the shot noise. So when Eq. (36) is satisfied, from Eq. (35), we can write

$$V_2 = |\bar{a}_o|^2 e^{-2}, \quad (37)$$

where V_2 is the power spectral density of noise due to the motion of atomic cell when Eq. (36) is satisfied.

V. RESULTS AND DISCUSSION

The total noise is given by shot noise, atomic noise and noise due to the mechanical motion of the atomic cell. Hence, the total noise can be obtained by from Eq. (30) and Eq. (37) as

$$N_o = \sqrt{V_1 + V_2} = \sqrt{|\bar{a}_o|^2} \sqrt{1 + 2e^{-2}}, \quad (38)$$

where N_o is the total noise when $\Omega^2 = \kappa\gamma_{bc}L$ and when Eq. (36) is satisfied. The minimum detectable angular velocity $\dot{\theta}_m := \dot{\theta}N_o/S_o$ is estimated as

$$\dot{\theta}_m = \frac{\nu c \gamma_{bc}}{4Q\dot{y}_o \omega_{cb}} \sqrt{\frac{\hbar \omega_p}{Pt_m}} \sqrt{1 + 2e^{-2}}, \quad (39)$$

where P is the power of the input probe field corresponding to the condition given in Eq. (36). Considering the realistic parameters such as $\dot{y}_o = 0.01$ m/s, $c = 3 \times 10^8$ m/s, $Q = 10^7$, $\nu = 1$ Hz, $\omega_{ab}/2\pi = 9 \times 10^{14}$ Hz, $\gamma_{bc} = 10^3$ Hz, $\hbar = 1.054 \times 10^{-34}$ J·s, $m = 1$ Kg, $t_m = 0.1$ s, $k_B = 1.38 \times 10^{-23}$ J/K, $N = 5 \times 10^{18}$ m⁻³ we estimate the quantum limit of minimum detectable rotation rate as $\dot{\theta}_m = 8.1 \times 10^{-19}$ rad/s at $P = 1.6$ Watt. At $T = 300$ K, the minimum detectable rotation rate is estimated as $\dot{\theta}_m = 2.3 \times 10^{-12}$ rad/s for $P = 2 \times 10^{-14}$ Watt.

From Eq. (39), we can improve the gyroscope's sensitivity by increasing \dot{y}_o . It is also possible to improve the sensitivity by decreasing γ_{bc} or by increasing Q , provided that the relation given Eq. (36) is maintained, otherwise the thermal noise from the mechanical oscillator can decrease the sensitivity. One may also wonder about the Fresnel-Fizeau dragging of light by the atomic medium. Especially, when a dispersive system like EIT system is considered [39–41]. However, according to Eq. (15), calculation in this manuscript is strictly limited to the linear dispersion case only. Hence the phase velocity of light inside the moving atomic cell is given as

$$\frac{c}{\chi(\omega_p - \dot{z}_m \frac{\omega_p}{c})} \approx \frac{c}{\chi(\omega_p)} + \dot{z}_m \frac{\omega_p}{\chi(\omega_p)^2} \frac{d\chi}{d\omega} \Big|_{\omega=\omega_p}. \quad (40)$$

When non-linear dispersion is neglected, and for $\chi(\omega) \approx 1$ (which is the case for EIT at two-photon resonance), the Fresnel-Fizeau dragging is equal to the second term on the RHS of Eq. (40).

Most of the modern navigation grade gyroscopes are based on the Sagnac effect [10, 42, 43]. Sagnac based RLG[7, 44] is limited by the line-width [45, 46] of the

laser field. Also, at very small rotations rates, cross-talk [45, 47] between the co-propagating and counter propagating laser modes reduces the accuracy of these gyroscopes. The sensitivity of FOG [48, 49] depends on the length of the optical path. Generally, high sensitivity is achieved in FOGs by passing the laser through a long optical fiber [50]. So the sensitivity of FOG is limited because of the scattering and absorption of light inside the optical fiber. Matter wave gyroscope has better sensitivity [51–54] when compared with FOG and ALG because of the short wavelength of matter wave in comparison with optical wave length. All the Sagnac effect based gyroscopes, like RLG, FOG, and matter wave gyroscopes, are dependent on the dimension of the Sagnac loop [55]. Unlike the Sagnac effect based gyroscopes, the atom-mechanical gyroscope do not depend on the dimensions. Quantum spin based rotation sensors have reached ultra-high sensitivity, however, these systems are difficult to commercialize. Conventional two-dimensional mechanical gyroscopes detect rotation by measuring Coriolis force. Radiation pressure force [56], which is exerted by the probe laser, limits the sensitivity of these systems. In the atom-mechanical gyroscope, the probe laser is almost transparent because of EIT and hence the radiation pressure force do not have any significant effect in this system.

A. Doppler broadening effect

Even when there is no rotation, at $\dot{\theta} = 0$, atoms inside the atomic cell are moving randomly in all directions with finite velocity because of thermal energy. This thermal motion, which is different from the Doppler effect arising due to rotation, leads to Doppler broadening effect. In this section we estimate the effect of thermal Doppler broadening. In presence of thermal motion, the $\bar{\sigma}_{ba}$ is given as

$$\bar{\sigma}_{baD}^{-1} = \frac{ig_c \bar{a} (i\omega_{cb} \frac{\dot{z}_m}{c} + i\Delta_3 - \gamma_{bc})}{(i\omega_{ab} \frac{\dot{z}_m}{c} + i\Delta_1 - \gamma_{ab})(i\omega_{cb} \frac{\dot{z}_m}{c} + i\Delta_3 - \gamma_{cb}) + |\Omega|^2}, \quad (41)$$

where $\Delta_1 = \omega_{ab}v_z/c$, $\Delta_3 = (\omega_{ab}v_z - (\omega_{ab} - \omega_{cb})v_y)/c$ represent the frequency detuning due to thermal Doppler effect. v_z and v_y are the velocity components of an atom along probe laser and drive laser, respectively, $\bar{\sigma}_{baD}^{-1}$ represents $\bar{\sigma}_{ba}$ in presence of thermal Doppler effect. Assuming that the cold atoms are at a temperature $T_a = 10^{-6}$ K, and have mass $m_a = 1.4 \times 10^{-25}$ Kg, the most probable velocity of an atom is given as $\sqrt{2k_B T_a/m_a} \approx 10^{-2}$ m/s. We estimate that $\Delta_1 \approx 10^5$ Hz and $\Delta_3 \approx 10^{-1}$ Hz for $\omega_{cb} = 10^{-6}\omega_{ab}$. Hence by using the approximation $\Omega^2 \gg \Delta_1\gamma_{bc} + \Delta_3\gamma_{ab} \gg \Delta_1\Delta_3$, Eq. (41) can be simplified as

$$\bar{\sigma}_{baD} \approx ig_c \bar{a} \left(\frac{i\Delta_3 - \gamma_{bc}}{|\Omega|^2} + i \frac{\omega_{cb} \dot{z}_m/c}{|\Omega|^2} \right). \quad (42)$$

Using the Maxwellian velocity distribution, Doppler broadening effect is estimated as

$$\frac{m}{2\pi k_B T} \int_{-\infty}^{\infty} \int_{-\infty}^{\infty} e^{-m(v_x^2 + v_y^2)/2k_B T} \bar{\sigma}_{baD} dv_y dv_z = \bar{\sigma}_{ba}. \quad (43)$$

Hence thermal Doppler effect is zero for the cold atoms. Note that the thermal motion of atoms is randomly directed in all directions and this leads to insignificant effect when integrated over all the possible directions. On the other hand, motion of the atom-mechanical oscillator due to Coriolis effect is non-random. Hence the velocity of the atom-mechanical oscillator due to the Coriolis force gives finite signal even in presence of thermal Doppler effect.

B. Effect of cooling lasers on atom-mechanical oscillator

Generally, cold atoms are prepared [57, 58] by reducing the atomic thermal kinetic energy by using a set of laser fields in all the three dimensions. So it is important to consider the effect of these cooling lasers on the velocity of atom-mechanical oscillator. The atom-mechanical is driven with velocity \dot{y} along Y-axis. We can fix the cooling laser set-up on the driving platform so the cooling lasers and the atom-mechanical are not moving with respect to each other along Y-axis.

Assuming that the cold atoms are at a temperature $T_a = 10^{-6}$ K and have mass $m_a = 1.4 \times 10^{-25}$ Kg, the most probable velocity of an atom is about 10^{-2} m/s. The maximum velocity of the atomic cloud due to the action of Coriolis force is

$$\int_0^{t_m} 2\dot{\theta}\dot{y} dt = \int_0^{t_m} 2\dot{\theta}\dot{y}_o \cos(\omega_m t) dt \approx 2\dot{y}_o \dot{\theta} t_m. \quad (44)$$

Substituting $\dot{y}_o = 10^{-2}$ m/s, $t_m = 0.1$ s, and $\dot{\theta} = 10^{-11}$ rad/sec, we note that the maximum velocity of atom-mechanical oscillator along Z-axis is about 10^{-14} m/s. Hence kinetic energy of atoms due to the Coriolis force is much smaller than the thermal kinetic energy of atoms and therefore the cooling lasers can not hinder the motion of the atom-mechanical oscillator due to the Coriolis force.

C. Effect of fluctuations in mechanical driving along Y-axis

In Eq. (8), we assumed that the mechanical drive along Y-axis is classical and it has no fluctuations. Such an approximation is accurate with in the linear regime for the following reason. Suppose that $\delta_{\dot{y}}$ is the fluctuation in the velocity of driving platform along Y-axis, then

Eq. (9) becomes

$$\dot{z}_m = \frac{2Q(\dot{y} + \delta_{\dot{y}})\dot{\theta}}{\nu} \cos(2\pi\nu t) + \frac{Q}{\nu} \hat{F}_{th}. \quad (45)$$

Both $\dot{\theta}$ and $\delta_{\dot{y}}$ are small and hence their product term can be neglected. Hence Eq. (45) reduces to Eq. (9) even when fluctuations along Y-axis are considered. Moreover, we are interested in measuring classical Coriolis force and hence it is reasonable to drop any fluctuation in the driving platform's velocity. Similarly we can also show that the thermal fluctuations in driving platform do not effect the rotation detection sensitivity. Given the recent progress in cooling[59–62] mechanical oscillators to their ground state, quantum limited sensitivity of 8×10^{-19} rad/s can be realized. Hence the method described in this work can be used to realize gyroscopes with very high sensitivities.

VI. CONCLUSION

Application of hybrid atom-mechanical system for absolute rotation detection is studied. Quantum noise limited sensitivity of the atom-mechanical gyroscope is estimated as 8×10^{-19} rad/s. For optimal performance of the gyroscope, the condition under which thermal noise from the mechanical oscillator can be set to the level of shot noise is derived. For the cold-atom set-up, assuming that the atoms are at $T_a = 10^{-6}$ K, the rotation detection sensitivity is estimated as 7×10^{-12} rad/s when the mechanical oscillator is at room temperature ($T = 300$ K).

VII. ACKNOWLEDGMENTS

This work is supported by the National Key R&D Program of China grant 2016YFA0301200 and the National Basic Research Program of China (under Grant No. 2014CB921403). It is also supported by Science Challenge Project (under Grant No. TZ2017003) and the National Natural Science Foundation of China (under Grants No. 11774024, No. 11534002, and No. U1530401)."

Appendix A: Many atom formalism

From Eq. (5), the equation for motion for the field mode \hat{c}_r is given as

$$\dot{\hat{c}}_r = -i\omega_r \hat{c}_r - ig^* \sum_s \sigma_{ba}^{ls} e^{-i(k_r - k_p)z_l}, \quad (A1)$$

By substituting $\omega_r = \omega_p + \frac{2r\pi c}{L_q}$ in Eq. (A1) and by taking summation on all the field modes, we can rewrite Eq. (A1) as

$$\begin{aligned}
&\Rightarrow \frac{\partial}{\partial t} \sum_r \hat{c}_r e^{i(k_r - k_p)z_l} = -i \sum_r \left(\omega_p + \frac{2r\pi c}{L_q} \right) \hat{c}_r e^{i(k_r - k_p)z_l} - i \sum_{r,s} g_r^* \sigma_{ba}^{ls}, \\
&\Rightarrow \frac{\partial}{\partial t} \sum_r \hat{c}_r e^{i(k_r - k_p)z_l} = -i \sum_r \left(\omega_p + c \frac{\partial}{\partial z_l} \right) \hat{c}_r e^{i(k_r - k_p)z_l} - i \sum_{r,s} g_r^* \sigma_{ba}^{ls}.
\end{aligned} \tag{A2}$$

By defining a new operator $\hat{c}_l(z_l, t)$ as

$$\hat{c}_l(z_l, t) = \sum_r \hat{c}_r e^{i(k_r - k_p)z_l},$$

Eq. (A2) can be rewritten as

$$\frac{\partial}{\partial t} \hat{c}_l(z_l, t) = -i\omega_p \hat{c}_l - c \frac{\partial}{\partial z_l} \hat{c}_l(z_l, t) - i \sum_{r,s} g_r^* \sigma_{ba}^{ls}. \tag{A3a}$$

Equations of motion for the atomic operators are

$$\dot{\hat{\sigma}}_{ba}^{ls} = (-i\omega_{ab} - \gamma_{ab}) \hat{\sigma}_{ba}^{ls} + i g_r (\hat{\sigma}_{aa}^{ls} - \hat{\sigma}_{bb}^{ls}) \hat{c}_l - i \tilde{\Omega} \hat{\sigma}_{bc}^{ls} + \hat{F}_{ba}^{ls}, \tag{A3b}$$

$$\dot{\hat{\sigma}}_{bc}^{ls} = (-i\omega_{cb} - \gamma_{bc}) \hat{\sigma}_{bc}^{ls} + i g_r \hat{\sigma}_{ac}^{ls} \hat{c}_l - i \tilde{\Omega}^* \hat{\sigma}_{ba}^{ls} + \hat{F}_{bc}^{ls}, \tag{A3c}$$

$$\dot{\hat{\sigma}}_{ac}^{ls} = (i\omega_{ac} - \gamma_{ac}) \hat{\sigma}_{ac}^{ls} + i(\hat{\sigma}_{cc}^{ls} - \hat{\sigma}_{aa}^{ls}) \tilde{\Omega}^* + i g_r^* \hat{\sigma}_{bc}^{ls} \hat{c}_l^\dagger + \hat{F}_{ac}^{ls}, \tag{A3d}$$

\hat{F}_{uv}^{ls} is the single atom noise operator. Assuming that the band-width of quasi-monochromatic probe field is much less than its mean frequency ω_p , we can write $\sum_r g_r = (2R+1)g$, with $g = \sqrt{\hbar\omega_p/\epsilon_0 A L_q}$. Hence Eq. (A3a) and Eq. (A2) can be written as

$$\frac{\partial}{\partial t} \hat{c}_l(z_l, t) = -i\omega_p \hat{c}_l - c \frac{\partial}{\partial z_l} \hat{c}_l(z_l, t) - i(2R+1) \sum_s g^* \sigma_{ba}^{ls}, \tag{A4a}$$

$$(2R+1) \sum_s \dot{\hat{\sigma}}_{ba}^{ls} = (-i\omega_{ab} - \gamma_{ab})(2R+1) \sum_s \hat{\sigma}_{ba}^{ls} + i g \sum_s (2R+1) (\hat{\sigma}_{aa}^{ls} - \hat{\sigma}_{bb}^{ls}) \hat{c}_l - \sum_s (2R+1) i \tilde{\Omega} \hat{\sigma}_{bc}^{ls} + \sum_s (2R+1) \hat{F}_{ba}^{ls}, \tag{A4b}$$

$$\sum_s (2R+1) \dot{\hat{\sigma}}_{bc}^{ls} = (-i\omega_{cb} - \gamma_{bc}) \sum_s (2R+1) \hat{\sigma}_{bc}^{ls} + i g \sum_s (2R+1) \hat{\sigma}_{ac}^{ls} \hat{c}_l - \sum_s (2R+1) i \tilde{\Omega}^* \hat{\sigma}_{ba}^{ls} + \sum_s (2R+1) \hat{F}_{bc}^{ls}, \tag{A4c}$$

$$\sum_s (2R+1) \dot{\hat{\sigma}}_{ac}^{ls} = (i\omega_{ac} - \gamma_{ac}) \sum_s (2R+1) \hat{\sigma}_{ac}^{ls} + \sum_s (2R+1) i (\hat{\sigma}_{cc}^{ls} - \hat{\sigma}_{aa}^{ls}) \tilde{\Omega}^* + i g^* \sum_s (2R+1) \hat{\sigma}_{bc}^{ls} \hat{c}_l^\dagger + \sum_s (2R+1) \hat{F}_{ac}^{ls}, \tag{A4d}$$

In the limit $R \rightarrow \infty$ or $\Delta z := z_{l+1} - z_l \rightarrow 0$, we go from discrete to continuous formulation by using the following transformations

$$z_l = \frac{lL_q}{2P+1} \rightarrow z, \tag{A5a}$$

$$\sum_{\omega_r} \rightarrow \frac{1}{\omega_{r+1} - \omega_r} \int d\omega, \tag{A5b}$$

$$\hat{c}_r \rightarrow \sqrt{\omega_{r+1} - \omega_r} \hat{c}(\omega) = \sqrt{\Delta\omega} \hat{c}(\omega) \tag{A5c}$$

$$\frac{2R+1}{N} \sum_s \hat{\sigma}_{ij}^{ls} \rightarrow \frac{2R+1}{N} \sum_s \hat{\sigma}_{ij}^{ls} |_{z_l \rightarrow z} := \hat{\sigma}_{ij}^o, \tag{A5d}$$

$$\frac{2R+1}{N} \sum_s \hat{F}_{ij}^{ls} \rightarrow \frac{2R+1}{N} \sum_s \hat{F}_{ij}^{ls} |_{z_l \rightarrow z} := \hat{F}_{ij}^o \tag{A5e}$$

$$\frac{\delta_{z,z'}}{z_{p+1} - z_p} = \frac{\delta_{z,z'}}{\Delta z} \rightarrow \delta(z - z'), \tag{A5f}$$

$$\frac{\delta_{\omega,\omega'}}{\omega_{r+1} - \omega_r} = \frac{\delta_{\omega,\omega'}}{\Delta\omega} \rightarrow \delta(\omega - \omega'). \tag{A5g}$$

Using Eq. (A5), we can write

$$\begin{aligned} \sum_r g_r \hat{c}_r e^{i(k_r - k_p)z_l} &= \sum_r g_r \hat{c}_r e^{i(k_r - k_p)z_l} e^{-i\omega_r t} \\ &\rightarrow \sqrt{\frac{\hbar\omega_p}{\epsilon_o A c}} \frac{1}{\sqrt{2\pi}} \int_0^\infty d\omega \hat{c}(\omega) e^{i(k - k_p)z} e^{-i\omega t} \\ &:= \sqrt{\frac{\hbar\omega_p}{\epsilon_o A c}} \hat{a} e^{-i\omega_p t}, \end{aligned} \quad (\text{A6})$$

We further defined a new operator \hat{a} which is normalized such that $\langle \hat{a}^\dagger \hat{a} \rangle$ represents the photons per unit time. By using Eq. (A6) and the relation $\sum_r g_r = (2R + 1)g$, Eq. (A4) can be transformed from discrete to continuous formalism. In the continuous notation, equations of motion are given as

$$\left(\frac{\partial}{\partial t} + c \frac{\partial}{\partial z} \right) \hat{a} = -iN \sqrt{\frac{c}{L_q}} g^* \hat{\sigma}_{ba}^o e^{i\omega_p t}, \quad (\text{A7a})$$

$$\dot{\hat{\sigma}}_{ba}^o = (-i\omega_{ab} - \gamma_{ab}) \hat{\sigma}_{ba}^o + i g_c (\hat{\sigma}_{aa}^o - \hat{\sigma}_{bb}^o) \hat{a} e^{-i\omega_p t} - i \tilde{\Omega} \hat{\sigma}_{bc}^o + \hat{F}_{ba}^o, \quad (\text{A7b})$$

$$\dot{\hat{\sigma}}_{bc}^o = (-i\omega_{cb} - \gamma_{bc}) \hat{\sigma}_{bc}^o + i g_c \hat{\sigma}_{ac}^o \hat{a} e^{-i\omega_p t} - i \tilde{\Omega}^* \hat{\sigma}_{ba}^o + \hat{F}_{bc}^o, \quad (\text{A7c})$$

$$\dot{\hat{\sigma}}_{ac}^o = (i\omega_{ac} - \gamma_{ac}) \hat{\sigma}_{ac}^o + i (\hat{\sigma}_{cc}^o - \hat{\sigma}_{aa}^o) \tilde{\Omega}^* + i g_c^* \hat{\sigma}_{bc}^o \hat{a}^\dagger e^{i\omega_p t} + \hat{F}_{ac}^o, \quad (\text{A7d})$$

After using rotating wave approximation by writing $\hat{\sigma}_{ba}^o = \hat{\sigma}_{ba} e^{-i\omega_p t}$ and $\hat{\sigma}_{ca}^o = \hat{\sigma}_{ca} e^{-i\omega_a t}$, we can write

$$\left(\frac{\partial}{\partial t} + c \frac{\partial}{\partial z} \right) \hat{a} = -iN g^* \sqrt{\frac{c}{L_q}} \hat{\sigma}_{ba}, \quad (\text{A8a})$$

$$\dot{\hat{\sigma}}_{ba} = [-i(\omega_{ab} - \omega_p) - \gamma_{ab}] \hat{\sigma}_{ba} + i g_c (\hat{\sigma}_{aa} - \hat{\sigma}_{bb}) \hat{a} - i \Omega \hat{\sigma}_{bc} + \hat{F}_{ba}, \quad (\text{A8b})$$

$$\dot{\hat{\sigma}}_{bc} = [-i(\omega_{cb} - (\omega_p - \omega_d)) - \gamma_{bc}] \hat{\sigma}_{bc} + i g_c \hat{\sigma}_{ac} \hat{a} - i \Omega \hat{\sigma}_{ba} + \hat{F}_{bc}, \quad (\text{A8c})$$

$$\dot{\hat{\sigma}}_{ac} = [i(\omega_{ac} - \omega_d) - \gamma_{ac}] \hat{\sigma}_{ac} + i (\hat{\sigma}_{cc} - \hat{\sigma}_{aa}) \Omega + i g_c^* \hat{\sigma}_{bc} \hat{a}^\dagger + \hat{F}_{ac}. \quad (\text{A8d})$$

-
- [1] C. W. F. Everitt, D. B. DeBra, B. W. Parkinson, J. P. Turneaure, J. W. Conklin, M. I. Heifetz, G. M. Keiser, A. S. Silbergleit, T. Holmes, J. Kolodziejczak, M. Al-Meshari, J. C. Mester, B. Muhlfelder, V. G. Solomonik, K. Stahl, P. W. Worden, W. Bencze, S. Buchman, B. Clarke, A. Al-Jadaan, H. Al-Jibreen, J. Li, J. A. Lipa, J. M. Lockhart, B. Al-Suwaidan, M. Taber, and S. Wang, *Phys. Rev. Lett.* **106**, 221101 (2011).
- [2] G. E. Stedman, *Reports on Progress in Physics* **60**, 615 (1997).
- [3] S. Smith, *Physics in Technology* **18**, 165 (1987).
- [4] D.-C. Lee and C.-S. Han, Proceedings of the Institution of Mechanical Engineers, Part B: Journal of Mechanical Engineering Science **223**, 1687 (2009), <http://pic.sagepub.com/content/223/7/1687.full.pdf+html>.
- [5] S. Ezekiel, *Optical Engineering* **13**, 136217 (1974).
- [6] H. J. Arditty and H. C. Lefevre, *Opt. Lett.* **6**, 401 (1981).
- [7] W. W. Chow, J. Gea-Banacloche, L. M. Pedrotti, V. E. Sanders, W. Schleich, and M. O. Scully, *Rev. Mod. Phys.* **57**, 61 (1985).
- [8] P. Berg, S. Abend, G. Tackmann, C. Schubert, E. Giese, W. P. Schleich, F. A. Narducci, W. Ertmer, and E. M. Rasel, *Phys. Rev. Lett.* **114**, 063002 (2015).
- [9] T. L. Gustavson, P. Bouyer, and M. A. Kasevich, *Phys. Rev. Lett.* **78**, 2046 (1997).
- [10] G. B. Malykin, *Physics-Uspekhi* **43**, 1229 (2000).
- [11] E. Kajari, R. Walsler, W. P. Schleich, and A. Delgado, in *Frontiers in Optics* (Optical Society of America, 2006) p. JWD48.
- [12] S. Davuluri and Y. Li, *New Journal of Physics* **18**, 103047 (2016).
- [13] S. Davuluri, K. Li, and Y. Li, *New Journal of Physics* **19**, 113004 (2017).
- [14] L. Kai, D. Sankar, and L. Yong, *SCIENCE CHINA Physics, Mechanics & Astronomy* (**accepted**), <https://doi.org/10.1007/s11464-017-0611-1>.
- [15] L. V. Hau, S. E. Harris, Z. Dutton, and C. H. Behroozi, *Nature* **397**, 594 EP (1999).
- [16] I. Novikova, R. Walsworth, and Y. Xiao, *Laser & Photonics Reviews* **6**, 333 (2012).
- [17] V. A. Sautenkov, H. Li, Y. V. Rostovtsev, and M. O. Scully, *Phys. Rev. A* **81**, 063824 (2010).
- [18] S. E. Harris, *Phys. Rev. Lett.* **62**, 1033 (1989).
- [19] H. R. Gray, R. M. Whitley, and C. R. Stroud, *Opt. Lett.* **3**, 218 (1978).
- [20] *Journal of Mechanical Engineering Science* **223**, 1687 (2009).
- [21] M. Fleischhauer, A. Imamoglu, and J. P. Marangos, *Rev. Mod. Phys.* **77**, 633 (2005).
- [22] M. Fleischhauer and M. O. Scully, *Phys. Rev. A* **49**, 1973 (1994).
- [23] S. Davuluri and Y. V. Rostovtsev, *EPL (Europhysics Letters)* **103**, 24001 (2013).
- [24] M. Aspelmeyer, T. J. Kippenberg, and F. Marquardt, *Rev. Mod. Phys.* **86**, 1391 (2014).
- [25] P. Meystre, *Annalen der Physik* **525**, 215 (2013).
- [26] M. Norgia and S. Donati, *Electronics Letters* **37**, 756 (2001).
- [27] T. Faust, J. Rieger, M. J. Seitner, J. P. Kotthaus, and E. M. Weig, *Nat Phys* **9**, 485 (2013), letter.
- [28] T. Faust, J. Rieger, M. J. Seitner, P. Krenn, J. P. Kotthaus, and E. M. Weig, *Phys. Rev. Lett.* **109**, 037205 (2012).
- [29] I. Abram, *Phys. Rev. A* **35**, 4661 (1987).
- [30] K. J. Blow, R. Loudon, S. J. D. Phoenix, and T. J.

- Shepherd, Phys. Rev. A **42**, 4102 (1990).
- [31] P. D. Drummond and S. J. Carter, J. Opt. Soc. Am. B **4**, 1565 (1987).
- [32] M. Fleischhauer and T. Richter, Phys. Rev. A **51**, 2430 (1995).
- [33] K. K. Das, G. S. Agarwal, Y. M. Golubev, and M. O. Scully, Phys. Rev. A **71**, 013802 (2005).
- [34] A. Dantan and M. Pinard, Phys. Rev. A **69**, 043810 (2004).
- [35] C. P. Sun, Y. Li, and X. F. Liu, Phys. Rev. Lett. **91**, 147903 (2003).
- [36] M. O. Scully and S. Zubairy, Quantum Optics, 1st ed. (Cambridge University Press, 1997).
- [37] I. Novikova, A. B. Matsko, V. L. Velichansky, M. O. Scully, and G. R. Welch, Phys. Rev. A **63**, 063802 (2001).
- [38] C. M. Caves, Phys. Rev. D **23**, 1693 (1981).
- [39] I. Carusotto, M. Artoni, G. C. La Rocca, and F. Bassani, Phys. Rev. A **68**, 063819 (2003).
- [40] S. Davuluri and Y. V. Rostovtsev, Phys. Rev. A **86**, 013806 (2012).
- [41] A. Safari, I. De Leon, M. Mirhosseini, O. S. Magaña Loaiza, and R. W. Boyd, Phys. Rev. Lett. **116**, 013601 (2016).
- [42] E. J. Post, Rev. Mod. Phys. **39**, 475 (1967).
- [43] G. B. Malykin, Physics-Uspekhi **40**, 317 (1997).
- [44] M. Faucheux, D. Fayoux, and J. J. Roland, Journal of Optics **19**, 101 (1988).
- [45] J. D. Cresser, W. H. Louisell, P. Meystre, W. Schleich, and M. O. Scully, Phys. Rev. A **25**, 2214 (1982).
- [46] W. Schleich, C. S. Cha, and J. D. Cresser, Phys. Rev. A **29**, 230 (1984).
- [47] J. D. Cresser, D. Hammonds, W. H. Louisell, P. Meystre, and H. Risken, Phys. Rev. A **25**, 2226 (1982).
- [48] H. C. Lefèvre, Optical Review **4**, A20 (1997).
- [49] V. Vali and R. W. Shorthill, Appl. Opt. **15**, 1099 (1976).
- [50] S. Schiller, Phys. Rev. A **87**, 033823 (2013).
- [51] M. O. Scully and J. P. Dowling, Phys. Rev. A **48**, 3186 (1993).
- [52] W. C. Campbell and P. Hamilton, Journal of Physics B: Atomic, Molecular and Optical Physics **50**, 063501 (2017).
- [53] S. Wu, E. Su, and M. Prentiss, Phys. Rev. Lett. **99**, 173201 (2007).
- [54] L. Qi, Z. Hu, T. Valenzuela, Y. Zhang, Y. Zhai, W. Quan, N. Waltham, and J. Fang, Applied Physics Letters **110**, 153502 (2017), <https://doi.org/10.1063/1.4980066>.
- [55] R. B. Hurst, J.-P. R. Wells, and G. E. Stedman, Journal of Optics A: Pure and Applied Optics **9**, 838 (2007).
- [56] C. M. Caves, Phys. Rev. Lett. **45**, 75 (1980).
- [57] T. Hnsch and A. Schawlow, Optics Communications **13**, 68 (1975).
- [58] D. J. Wineland, R. E. Drullinger, and F. L. Walls, Phys. Rev. Lett. **40**, 1639 (1978).
- [59] O. Arcizet, P.-F. Cohadon, T. Briant, M. Pinard, A. Heidmann, J.-M. Mackowski, C. Michel, L. Pinard, O. François, and L. Rousseau, Phys. Rev. Lett. **97**, 133601 (2006).
- [60] F. Marquardt, J. P. Chen, A. A. Clerk, and S. M. Girvin, Phys. Rev. Lett. **99**, 093902 (2007).
- [61] M. Bhattacharya and P. Meystre, Phys. Rev. Lett. **99**, 073601 (2007).
- [62] A. Schliesser, R. Riviere, G. Anetsberger, O. Arcizet, and T. J. Kippenberg, Nat. Phys. **4**, 415 (2008).